PREDICTION OF SWELLING CHARACTERISTICS OF COMPACTED GMZ BENTONITE IN SALT SOLUTION INCORPORATING ION-EXCHANGE REACTIONS

Guosheng Xiang[1,2], Yongfu Xu[2], Feng Yu[1]*, Yuan Fang[1]*, and Yi Wang[1]

[1]Department of Civil Engineering, Anhui University of Technology, Maanshan 243002 Anhui, China
[2]School of Naval Architecture, Ocean & Civil Engineering, Shanghai Jiao Tong University, Shanghai 200240, China

Abstract—Salt solutions have complex effects on the swelling characteristics of compacted bentonite; these effects are caused by the inhibitory action of salinity and the ion-exchange reaction between the solution and bentonite. In order to characterize the swelling properties of compacted bentonite in a salt solution, swelling deformation tests were carried out for Gao-Miao-Zi (GMZ) bentonite specimens in NaCl and CaCl$_2$ solutions. Swelling characteristics decreased with increasing salt concentration. Swelling strains in NaCl solution were larger than those in CaCl$_2$ solution, even though the ionic concentration of 1.0 mol/L (M) NaCl solution is larger than that of 0.5 M CaCl$_2$. According to the exchangeable cations tests, cation exchange was different for specimens immersed in different salt solutions. The swelling fractal model was used to predict the swelling strains of compacted bentonite in a concentrated salt solution. In this model, the effective stress incorporating osmotic suction was applied to take the effect of salinity into consideration, and the swelling coefficient, K, was employed to describe the swelling properties affected by the variation in exchangeable cations. In the model, fractal dimension was measured by nitrogen adsorption, and the salt solution had little effect on fractal dimension. K was estimated by the diffuse double layer (DDL) model for osmotic swelling in distilled water. Comparison of fractal model estimations with experimental data demonstrated that the new model performed well in predicting swelling characteristics affected by a salt solution.

Keywords—Bentonite · Fractal Model · Ion-exchange Reaction · Salt Solution · Swelling Characteristics

INTRODUCTION

Bentonite is recognized generally as an ideal buffer/backfill material for artificial barriers in deep geological repositories for nuclear waste due to its low hydraulic conductivity, high swelling characteristics, and good self-sealing capacity (Karnland et al. 2007; Dohrmann et al. 2013; Sellin and Leupin 2013; Sun et al. 2015; Chen et al. 2016; Kaufhold and Dohrmann 2016). Bentonite can fill cracks between bentonite and the surrounding crystalline rock to form an enclosed environment, effectively restricting nuclide migration. During the operation of a repository, however, groundwater solution may infiltrate into and thereby affect the swelling properties of the buffer/backfill material. The effect of saline groundwater on the swelling characteristics of bentonite is expressed mainly in two aspects. First of all, the salinity of groundwater has a strong inhibitory effect on swelling potential (Villar 2006; Siddiqua et al. 2011). This relationship can be explained by DDL theory as the spacing between clay particles decreases with an increase in ion concentration in the pore water. Secondly, the variation of cations adsorbed by bentonite also affects swelling characteristics (Segad et al. 2012a, b; Liu 2013).

Montmorillonite is regarded as the only component in bentonite responsible for water uptake and swelling processes. A plate-like montmorillonite layer is ~0.96 nm thick. Montmorillonite plates often combine in a face-to-face orientation (Saiyouri et al. 2004). The face of the montmorillonite layer has a permanent negative charge resulting from isomorphous substitutions of divalent cations (e.g. Mg^{2+} and Fe^{2+}) for trivalent Al^{3+} in the octahedral sheet and trivalent Al^{3+} for tetravalent Si^{4+} in the tetrahedral sheet. This charge is compensated by the preferential adsorption of cations on the layer surface, such as Na$^+$, K$^+$, Ca^{2+}, or Mg^{2+}, which commonly, are hydrated and exchangeable. If the cations in salt solutions are significantly different from the exchange population present on the exchange sites, a cation exchange reaction will occur.

The swelling phase of compacted bentonite specimens may be divided into two dominant processes: crystalline swelling and osmotic swelling (Liu 2013). In crystalline swelling, water molecules are inserted between the unit layers caused by hydration of the interlayer cations (Holmboe et al. 2010; Siddiqua et al. 2011; Ferrage 2016; Birgersson 2017). Four discrete layers of water molecules exist in a Na-montmorillonite, while less than 3 layers are present in other cationic montmorillonites (Yong 1999; Liu 2013). Upon further water infiltration, the distance between montmorillonite layers increases gradually, the hydrated cations deviate from the outer montmorillonite surfaces into the interparticle pore space, and the DDLs begin to form on the clay surface. This phase is

called the osmotic swelling phase. Ca-montmorillonite particles may divide into stacks of 2–20 unit layers depending on the pore water salinity and other experimental conditions. Na-montmorillonite can divide into smaller stacks of 1–5 unit layers (Cadene et al. 2005; Segad et al. 2012a, b), suggesting a higher swelling potential for Na-montmorillonite than its calcium counterpart. Thus, the ion-exchange reaction between cations existing in groundwater and that adsorbed on exchange positions on the layer surface may also change the swelling characteristics greatly (Schramm and Kwak 1982a, b; Segad et al., 2012a, b).

Due to the effects of salt solution on the swelling of bentonite being very complex, few methods can predict accurately the swelling characteristics of bentonite in a salt solution. The DDL model was found to be suitable in predicting osmotic swelling of compacted bentonites in a dilute salt solution (Tripathy et al. 2004; Xiang et al. 2014). However, this model has limitations in estimating crystalline swelling and is not suitable for specimens in concentrated solution (Yong 1999; Liu 2013). Rao and Thyagaraj (2007) pointed out that an increase in salt concentration of pore fluid leads to an increase in osmotic suction, which acts as an additive effective stress component leading to a decline in swelling potential. Based on fractal analyses of bentonite micro-structures, the effective stress incorporated with osmotic suction was expressed by Xu et al. (2014), and the correlation of montmorillonite void ratio (e_m) with effective stress (p_e) conforms to a fractal model with $e_m = K p_e^{D_s-3}$, where K is the swelling coefficient of montmorillonite and D_s is the surface fractal dimension. This model can be used to describe the swelling behavior affected by the salinity of pore water. The effect of a salt solution incorporating ion-exchange reactions has not been well studied, however. Especially, a comprehensive theoretical description of the influence of swelling characteristics of compacted bentonite in salt solution is lacking.

The objectives of the present work were: (1) to investigate the influence factors of different salt solutions on swelling strain; (2) to calculate the effect of exchange reactions on swelling strain; and (3) to predict the swelling strains of compacted bentonite in a concentrated salt solution.

PREDICTIVE MODEL

As mentioned above, the correlation of montmorillonite void ratio to effective stress was satisfied by the swelling fractal model. The effective stress on bentonite particles is defined generally as the net interaction force between soil particles, and in the case of montmorillonite swelling, effective stress can be regarded as the interaction force between montmorillonite layers. When compacted specimens are in contact with distilled water, the effective stress is balanced by the vertical pressure, σ, applied in swelling tests, without the osmotic suction of pore water. While in a salt solution, the effective stress, p_e, of compacted bentonite exposed to osmotic suction could be represented as (Xu et al. 2014; Xiang

et al. 2016):

$$p_e = \sigma + \pi \left(\frac{\sigma}{\pi}\right)^{D_s-2} \tag{1}$$

where σ is vertical overburden pressure applied on the specimen, π is osmotic suction of pore water and can be expressed as (Rao and Thyagaraj 2007):

$$\pi = iMRT \tag{2}$$

where M is the molar concentration of the salt solution, R is the universal gas constant, T is absolute temperature in Kelvin, and i is the Van't Hoff factor and equals to 2 and 3 for the sodium chloride and calcium chloride solutions, respectively (Rao and Shivananda 2005). The $CaCl_2$ solution, therefore, has 1.5 times the osmotic suction of the NaCl solution at the same molar concentration.

By incorporating osmotic suction in effective stress, the fractal model provides an effective method to express the effect of pore-water salinity on swelling characteristics of compacted bentonite. The swelling coefficient of montmorillonite, K, is an inherent parameter of montmorillonite, and is independent of the salinity of pore water. As mentioned above, in addition to pore-water salinity, the main factors influencing the swelling behavior of montmorillonite are the surface charge density and the cations adsorbed on exchange positions on the layer surface. Due to the fact that the salt solution usually does not participate in isomorphous substitutions, the surface charge density is basically unchanged. However, cations on the exchange positions would be exchanged via the ion-exchange reaction. The influence of changes in exchangeable cations on swelling characteristics is reasonably described by the swelling coefficient K (Xiang et al. 2014).

The DDL model was suitable in predicting osmotic swelling of bentonites in distilled water (Liu 2013). Thus, the coefficient K can be estimated on the assumption that the fractal equation should be equivalent to the DDL model in the case of osmotic swelling in distilled water. Rearranging the fractal model gives

$$K = e_m p_e^{3-D_s} \tag{3}$$

According to the DDL model, the effective stress, p_e, and the montmorillonite void ratio, e_m, can be calculated by the average distance, d_m, between the 2:1 montmorillonite layers (Fig. 1), i.e. the distance from the top of a montmorillonite layer to the bottom of the one directly above it. Osmotic swelling is assumed generally to follow the completion of crystalline swelling. Thus, the distance d should be larger when crystalline swelling has fully taken place. Osmotic swelling was assumed to develop to such an extent that the montmorillonite particles cannot divide into small stacks (Fig. 1). The

separation distance between the montmorillonite particles was given by h, the particles consist of n_s, the number of montmorillonite layers, and the unit montmorillonite layers were separated by an interlayer distance d_m. The value of e_m for montmorillonite is then related to h as (Liu 2013):

$$h = n_s t e_m - (n_s - 1) d_m \qquad (4)$$

where t is the thickness of a montmorillonite layer and d_m should be taken as a weighted average of separation distance because it depends on the types of exchangeable cations, and is defined as

$$d_m = \frac{1}{CEC} \sum_i EXC_i d_i \qquad (5)$$

where CEC is the cation exchange capacity of bentonite and EXC_i is the exchange capacity of the ith exchangeable cation, and d_i is the fixed distance between unit montmorillonite layers when only the ith exchangeable cation is present. It is approximated by $d_i = 1.2$, 0.6, and 0.9 nm for Na-, K-, and Ca- (or Mg-) montmorillonites, respectively (Yong 1999; Liu 2013).

The montmorillonite void ratio e_m can be expressed as:

$$e_m = \frac{d - R_{ion}}{t + R_{ion}} \qquad (6)$$

where d is half of the average distance between the montmorillonite layers and R_{ion} is the radius of unhydrated exchangeable cations and is used as the weighted average to take into account the demixing of cations

$$R_{ion} = \frac{1}{CEC} \sum_i EXC_i R_i \qquad (7)$$

where R_i is radius of ith exchangeable cation.

Combining Eqs. 4 and 6, if osmotic swelling takes place, indicates that h should be larger than d_m and the distance d should satisfy:

$$d > \frac{t + R_{ion}}{t} d_m + R_{ion} \qquad (8)$$

Once the value of d_m is obtained, K can be calculated from Eq. 3 if p_e is known. The value of p_e is given by the DDL theory (Bolt 1956) as:

$$p_e = f_r - f_a \qquad (9)$$

where f_r is the repulsive force and f_a is the Van der Waals attractive force, which is expressed by the Hamaker's equation (Casimir and Polder 1948; Liu and Neretnieks 2008):

$$f_a = \frac{A_h}{6\pi} \left[\frac{1}{d^3} - \frac{2}{(d+t)^3} + \frac{1}{(d+2t)^3} \right] \qquad (10)$$

where A_h is the Hamaker constant (J).

Repulsive pressure f_r is given by the Gouy-Chapman theory (Bolt 1956; Iwata et al. 1988)

$$f_r = 2n_0 kT (\cosh u - 1) \qquad (11)$$

where n_0 is the concentration of ions in pore water, k, is the Boltzmann's constant, T is the absolute temperature, u is the electrostatic potential at the mid-plane between parallel
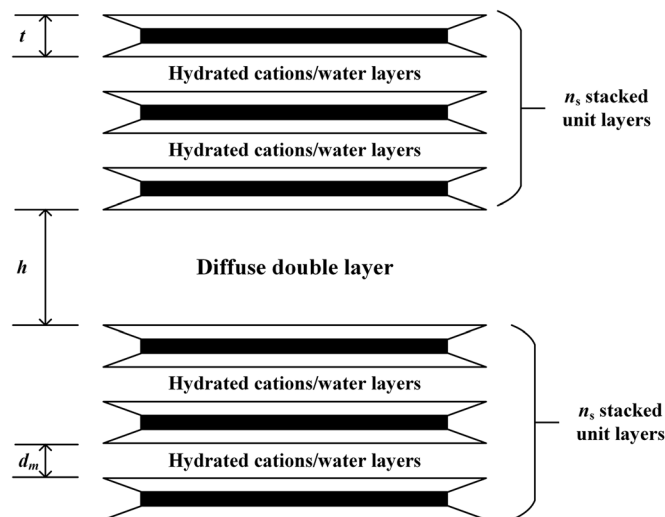

Fig. 1 A schematic representation of osmotic swelling with a diffuse double-layer existing between montmorillonite particles (Liu 2013)

montmorillonite layers, and is described as (Iwata et al. 1988; Liu 2013):

$$u = \sinh^{-1}[2\sinh u_m + (4/\kappa d)\sinh(u_h/2)] \quad (12)$$

where the two scaled potentials on the right-hand side are for the isolated particles and can be written explicitly as (Iwata et al. 1988; Liu and Neretnieks 2008):

$$u_m = 4\tanh^{-1}[\exp(-\kappa d/2)\tanh(z/4)] \quad (13)$$

and

$$u_h = 4\tanh^{-1}[\exp(-\kappa d)\tanh(z/4)] \quad (14)$$

In these expressions, κ is the reciprocal Debye length (Iwata et al. 1988):

$$\kappa = \sqrt{\frac{2n_0 \nu^2 e'^2}{\varepsilon k T}} \quad (15)$$

z is the scaled surface-potential of the isolated particle, and is described as (Iwata et al. 1988; Liu 2013):

$$z = 2\sinh^{-1}\left(96.5 \times \frac{\text{CEC}}{S}\sqrt{\frac{1}{8\varepsilon n_0 k T}}\right) \quad (16)$$

where e' is the charge on the electron, ε is the static permittivity of pore water, S is the total specific surface area of bentonite, and ν is the average valence of exchangeable cations. In the case involving a mixture of several types of exchangeable cation, a simple method to apply the DDL model in the evaluation of p_e is to define υ as the weighted average valency of exchangeable cations,

$$\nu = \frac{1}{\text{CEC}}\sum_i \text{EXC}_i \nu_i \quad (17)$$

It is important to note that predicting swelling characteristics of compacted bentonite using this method is based on the temperature, which is assumed to be static and uniform throughout the swelling system. In a real bentonite barrier of deep geological repositories, temperatures will be higher and there will be a temperature gradient (Åkesson et al. 2009; Zheng et al. 2015; Villar et al. 2016). In such circumstances, the proposed method may be of doubtful utility for estimating swelling characteristics.

MATERIAL AND METHODS

Materials

GMZ bentonite was taken from the Inner Mongolia Autonomous Region, 300 km northwest of Beijing, China. GMZ bentonite has been selected as a potential buffer/backfill material for the artificial barrier in the Chinese program of deep geological repositories. The typical properties of GMZ bentonite are given in Table 1 (Chen et al. 2014; Ye et al. 2014, 2015). It contains ~74% montmorillonite, 11.7% quartz, 4.3% feldspar, 7.3% calcite, and very small amounts of kaolinite and illite (Sun et al. 2013).

For swelling deformation, distilled water (DW), 0.5 M NaCl (0.5 Na), 1.0 M NaCl (1.0 Na), 0.5 M CaCl$_2$ (0.5 Ca), and 1.0 M CaCl$_2$ (1.0 Ca) solutions were used as the immersing reagents.

Swelling characteristics tests

GMZ bentonite powder was first mixed with distilled water, by means of a spray during mixing, to a water content of 18.0%, and then placed in a sealed container at room temperature for 48 h. The wet bentonite was compacted to cylindrical specimens of diameter 60 mm, height 10 mm. The initial dry density of the specimens was controlled at 1.60 or 1.70 g/cm^3. Compaction was performed at a constant loading rate of 0.2 kN/min using a digital press. The applied load and displacements of the piston were recorded by a load cell and a digital gauge, respectively. When the target density was reached, the maximum load was maintained for 1 h for homogenization of the sample.

After compaction, the bentonite specimen was placed into an oedometer (Fig. 2), and a specified vertical pressure (50, 100, 200, 400, or 800 kPa) was applied. Distilled water or salt solution was then supplied to the oedometer, allowing the liquid level to rise gradually until the specimen was submerged completely. The swelling deformation of the specimens was recorded by a strain gauge with a precision of 0.001 mm. Specimens were considered stabilized when the reading on the dial held constant for 24 h. The equilibration time for various specimens was ranged over ~20–30 days. The swelling strain, ε_s, was defined as the percentage of change in the specimen's height, and the maximum swelling strain (ε_{max}) was defined as swelling strain at the final swelling state.

Exchangeable cations tests

After swelling in salt solution, the compacted specimens were unloaded; each time ~15 g of the tested bentonite was stirred in 1000 mL of water for 5 min and filtered with qualitative filter paper with a pore size of 11 μm. This process

Table 1 Physical properties of GMZ bentonite

Physical properties	Value
Specific gravity	2.66 mg/m^3
Liquid limit	276%
Plastic limit	37%
Plasticity index	239
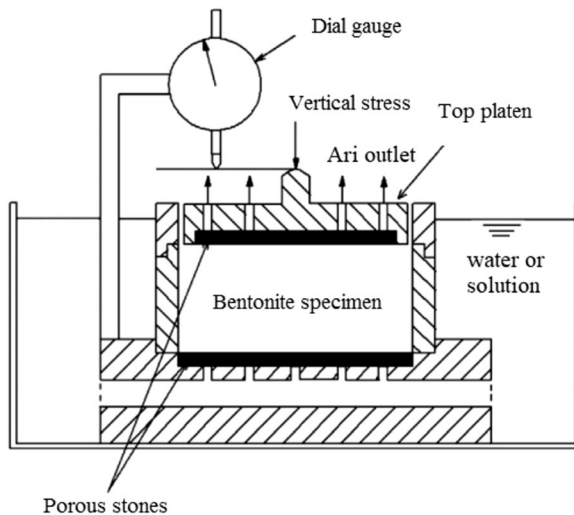
Fig. 2 Schematic diagram of oedometer used in swelling deformation tests (Sun et al. 2013)

Table 2 Exchangeable cation compositions of natural GMZ bentonite equilibrated with various solutions at room temperature for ~20–30 days

Equilibrating solution*	Exchangeable cation (cmol(+)/kg)			
	Na^+	Ca^{2+}	Mg^{2+}	K^+
DW	36.2	24.7	11.9	2.3
0.5 Na	38.8	23.1	10.9	2.2
1.0 Na	40.3	22.3	10.1	2.0
0.5 Ca	32.8	29.9	10.0	2.1
1.0 Ca	28.8	34.9	9.1	2.0

*DW: distilled water, 0.5 Na: 0.5 M NaCl, 1.0 Na: 1.0 M NaOH, 0.5 Ca: 0.5 M CaCl2, 1.0 Ca: 1.0 M $CaCl_2$

was repeated twice in water and twice in 95% alcohol in order to wash the salt from the pores. Together with specimens in distilled water, samples were oven dried at 105°C for 24 h, homogenized, and passed through a 0.03 mm sieve for exchangeable cations tests.

Exchangeable cations were removed by the ammonium displacement method standardized in ASTM D7503 (ASTM 2010) and exchangeable cations values were measured using ICP-MS Quadrupole Nexion instrument (PerkinElmer, Boston, Massachusetts, USA) analysis processed by Analysis and Testing Center of Shanghai Jiaotong University. In each salt solution, the exchangeable cation values of five specimens tested were averaged. Only Na^+, K^+, Mg^{2+}, and Ca^{2+} were taken into consideration.

Nitrogen adsorption tests

The nitrogen adsorption test is used commonly to study the surface fractality of bentonite (Celis et al. 1998; Xiang et al. 2016; Xu 2018). In the present study, the nitrogen adsorption test

was performed in order to measure the surface fractal dimension using an ASAP-2020 M surface analyzer (Micromeritics, Norcross, Georgia, USA) at 77 K. The same pretreatment of specimens as described in the exchangeable cations tests was also carried out before the nitrogen adsorption test.

RESULTS

Maximum Swelling Strain

The maximum swelling strain was heavily dependent on the initial dry density, vertical pressure, and salt solution (Fig. 3).

(1) The greater the initial dry density, the greater the swelling strain for specimens in the same solution under the same vertical overburden pressure.

(2) At the same initial dry density, the swelling strain decreased with the vertical pressure for specimens in contact with the same solution.

(3) Under the same vertical overburden pressure, the swelling strain of the specimens decreased with the concentration of the salt solution because the effective stress was
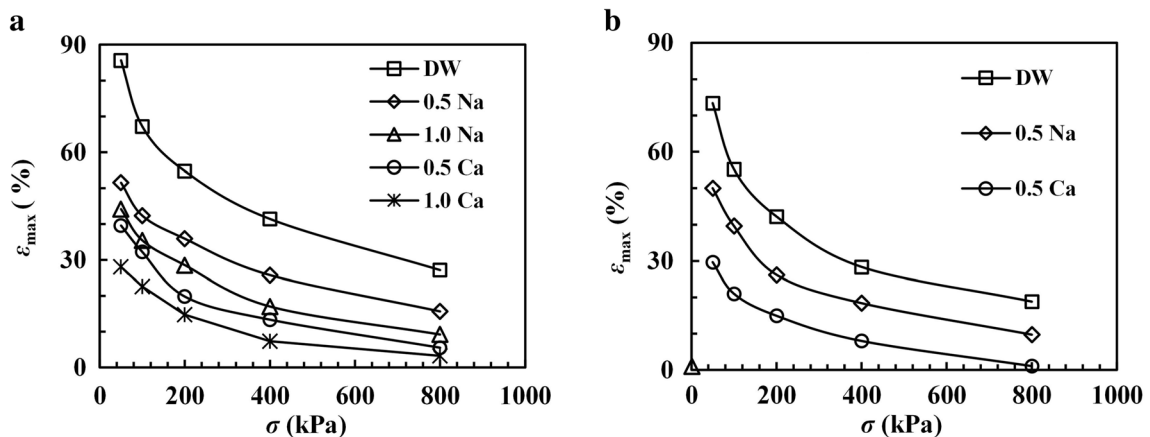

Fig. 3 Maximum swelling strain vs. vertical pressure of specimens in various aqueous solutions with an initial dry density of (**a**) 1.7 g/cm³ and **b** 1.6 g/cm³

increased by the increase in osmotic suction of pore water.

(4) Due to the CaCl$_2$ solution having 1.5 times the osmotic suction of the NaCl solution at the same molar concentration, the swelling strains of specimens in 0.5 M CaCl$_2$ solution were always smaller than those of specimens in 0.5 M NaCl solution.

(5) The swelling strains of specimens in 0.5 M CaCl$_2$, however, were also smaller than those of specimens in 1.0 M NaCl solution, which may imply that an ion-exchange reaction occurs between compacted specimens and the inundating solution and has a significant influence on the swelling potential.

Table 3 Non-hydrated radius of typical ions (Liu 2013)

Ion	Non-hydrated radius (nm)	R_i (nm)
Na$^+$	0.098	0.098
K$^+$	0.133	0.133
Mg^{2+}	0.078–0.089	0.0835
Ca^{2+}	0.106–0.117	0.1115

Exchangeable Cations

The results from the measurement of exchangeable cations (Table 2) showed that the exchangeable Na$^+$ values increased
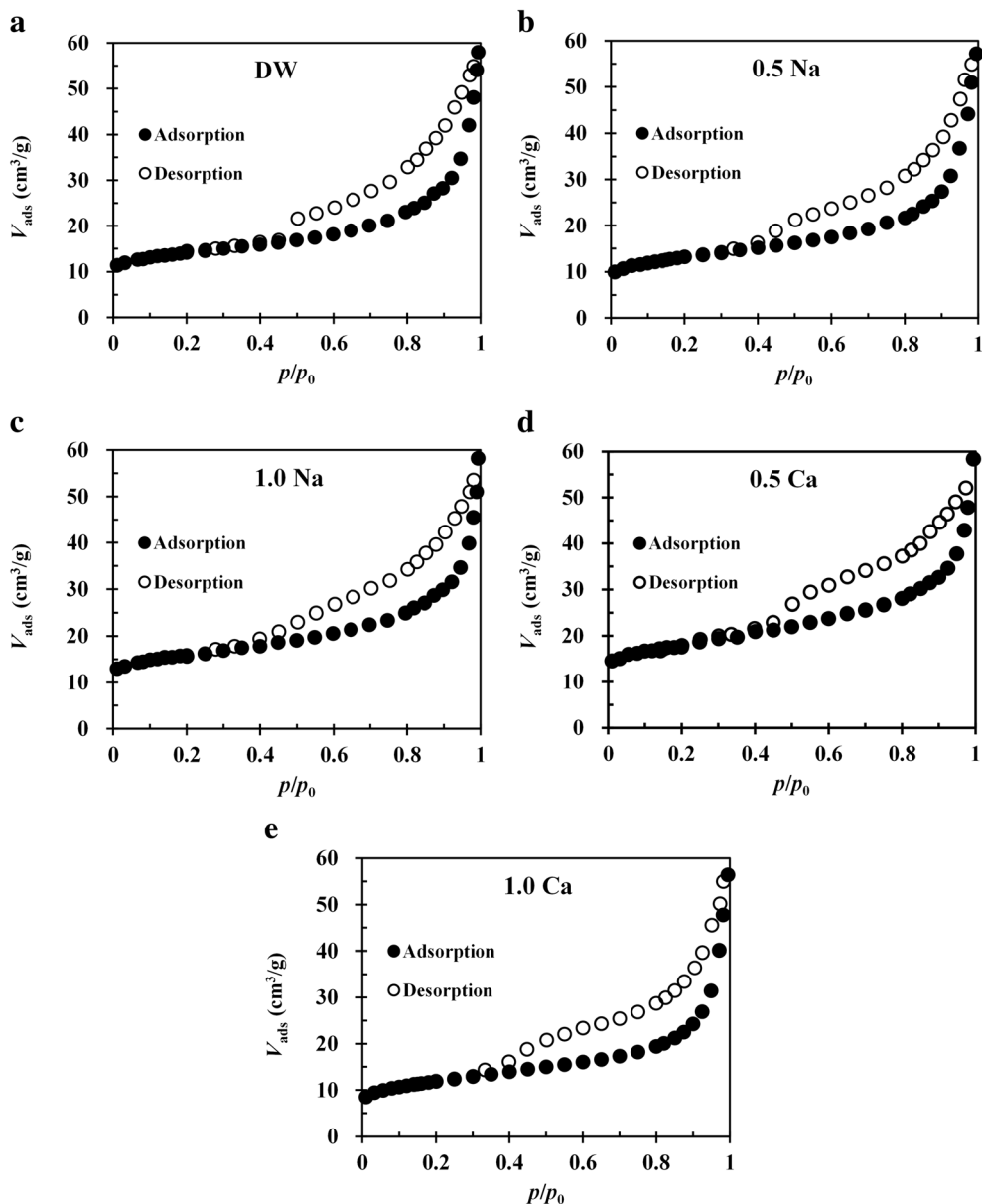

Fig. 4 Nitrogen adsorption–desorption isotherms of bentonite specimens in (**a**) distilled water, (**b**) 0.5 M NaCl, (**c**) 1.0 M NaCl, (**d**) 0.5 M CaCl$_2$, and (**e**) 1.0 M CaCl$_2$ solution

Table 4 Physical parameters for determination of K

Parameters	Notation	Value
Absolute temperature	T	298 K
Boltzmann constant	k	1.38×10^{-23} J/K
Hamaker constant	A_h	2.2×10^{-20} J
Static permittivity of pore water	ε	$78.54 \times 8.8542 \times 10^{-12}$ C^2/J/m
Charge on the electron	e'	1.602×10^{-19} C
Thickness of montmorillonite layer	t	0.96 nm
Ion concentration of pore water	n_0	$10 \times 6.023 \times 10^{23}$ ions/m^3
Total specific surface area of GMZ bentonite	S	0.74×810 m^2/g

while other exchangeable cations decreased simultaneously for specimens in contact with a NaCl solution, suggesting that Na$^+$ exchanged with other exchangeable cations on the montmorillonite surface. Similarly, for specimens in contact with CaCl$_2$ solution, the Ca^{2+} replaced other exchangeable cations, which resulted in an increase of exchangeable Ca^{2+} values and decrease in Na$^+$ and Mg^{2+}. And the extent of ion exchange was greater when using more concentrated salt solutions.

Surface Fractal Dimension

The nitrogen adsorption-desorption isotherms of all bentonite specimens had a hysteresis loop (Fig. 4), suggesting the adsorption process was dominated by capillary condensation. The nitrogen adsorption isotherms of bentonite specimens can be analyzed by the Frenkel-Halsey-Hill equation which was expressed as (Avnir and Jaroniec 1989):

$$V_{\text{ads}} = A[\ln(p_0/p)]^{3-D_s} \qquad (18)$$

where A is a constant, V_{ads} is the gas volume adsorbed at equilibrium pressure p, p_0 is the saturation pressure of the adsorbate, and D_s is surface fractal dimension of bentonite specimens.

The global adsorption process ($p/p_0 = 0.01–0.99$) was adopted to estimate the D_s values, which were estimated for all specimens as ~2.74, the value for the compacted specimen in distilled water.

PREDICTION AND COMPARISONS

Before prediction of the swelling deformation of bentonite in various salt solutions, the swelling coefficient K should be calculated. As mentioned above, the K value can be calculated by the DDL model in the case of osmotic swelling, where the distance d should satisfy Eq. 8. The radius of typical exchangeable cations is listed in Table 3; combined with the exchangeable cation compositions of bentonite specimens swollen in various different solutions (Table 2), the value of d of each specimen should be >1.2 nm. In addition, previous research indicated that larger values of d would appear in the bentonite specimens with higher exchangeable Na$^+$, where osmotic swelling has been fully developed (Saiyouri et al. 2004; Ferrage et al. 2007; Liu 2013). The values of d from different specimens varied, therefore, according to the exchangeable cation composition (Table 2). The physical parameters (Table 4), taken from the literature (Liu 2013; Xiang et al. 2014), were then used to calculate the swelling coefficient, K, (Table 5), which indicated clearly that K increased directly with the exchangeable Na$^+$ content.

Table 5 Variables used in the calculation of the swelling coefficient, K, for different exchangeable cation compositions of compacted bentonite

Solution	d (nm)	e_m	u_h	u_m	u	f_r (kPa)	f_a (kPa)	p_e (kPa)	K
DW	1.5	1.32	1.87	2.96	3.92	1194.32	218.20	976.11	6.88
0.5 Na	1.6	1.41	1.80	2.89	3.85	1110.99	172.58	938.41	7.30
1.0 Na	1.7	1.51	1.73	2.82	3.77	1021.70	138.14	883.55	7.67
0.5 Ca	1.4	1.22	1.93	3.02	3.98	1274.22	279.65	994.57	6.03
1.0 Ca	1.3	1.12	1.99	3.07	4.04	1361.83	363.99	997.84	5.74

d is half of the average distance between the montmorillonite layers, e_m is the montmorillonite void ratio, u_h and u_m are the two scaled potentials on the right-hand side are for the isolated particles, u is the electrostatic potential at the mid-plane between parallel montmorillonite layers, f_r is the repulsive force, f_a is the Van der Waals attractive force, and p_e is the effective stress

Table 6 Comparison of predicted montmorillonite void ratio with measured values ($\rho_d = 1.7$ g/cm^3)

		50 kPa	100 kPa	200 kPa	400 kPa	800 kPa
DW	ε_{max} (%)	85.65	67.24	54.81	41.46	27.19
	e_m (measured)	2.70	2.30	2.03	1.74	1.43
	e_m (predicted)	2.70	2.28	1.93	1.64	1.39
0.5 Na	ε_{max} (%)	51.59	42.38	35.94	25.81	15.69
	e_m (measured)	1.96	1.76	1.62	1.40	1.18
	e_m (predicted)	2.11	1.84	1.60	1.39	1.20
1.0 Na	ε_{max} (%)	44.99	34.28	24.86	16.57	9.30
	e_m (measured)	2.71	2.89	3.12	3.44	3.95
	e_m (predicted)	1.80	1.61	1.46	1.21	1.04
0.5 Ca	ε_{max} (%)	41.20	30.94	21.91	13.98	7.02
	e_m (measured)	1.71	1.49	1.30	1.13	0.98
	e_m (predicted)	1.70	1.54	1.27	1.13	0.96
1.0 Ca	ε_{max} (%)	27.74	19.28	11.84	5.29	−0.47
	e_m (measured)	1.50	1.31	1.14	0.99	0.86
	e_m (predicted)	1.45	1.33	1.16	1.00	0.91

Once the swelling coefficient K is obtained, the swelling deformation of specimens in salt solution can be predicted by the fractal model. The relationship between ε_{max} of bentonite and e_m at full saturation can be written as (Xu, Matsuoka and Sun 2003)

$$\varepsilon_{smax} = \left(\frac{C_m \rho_b / \rho_m e_m + 1}{\rho_b} \rho_{d0} - 1 \right) \times 100\% \qquad (19)$$

where C_m is the montmorillonite content in bentonite, ρ_b is the specific gravity of bentonite, ρ_m is the specific gravity of montmorillonite, and ρ_{do} is the initial dry density.

The measured montmorillonite void ratio can be obtained from Eq. 19. The montmorillonite void ratio of specimens with 1.7 g/cm^3 initial dry density was estimated by the fractal model (Table 6), as the swelling coefficient, K, was obtained, and the effective stress, p_e, was calculated incorporating the osmotic suction of the inundating solution. Good agreement was found between the predicted montmorillonite void ratio and the measured values. Experimental data of GMZ bentonite in distilled water and NaCl solution from Ye et al. (2014) were also plotted for comparison (Fig. 5). Predicted values agreed well with experimental results for the relationship between the montmorillonite void ratio and the applied load.

The swelling strain of bentonite in salt solution can also be predicted (Fig. 6). The estimations of maximum swelling strain also fitted well with experimental data.
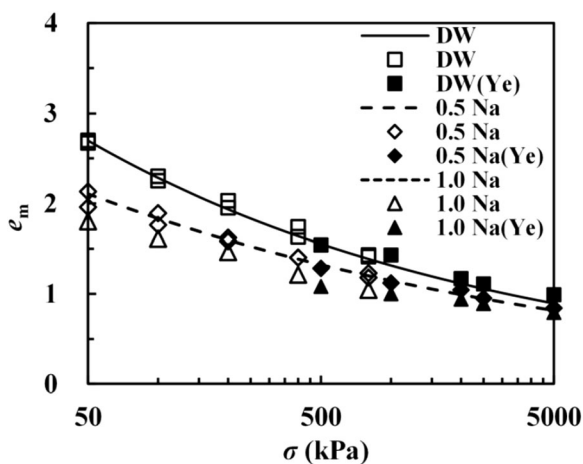

Fig. 5 Comparison of measured montmorillonite void ratio with the predicted void ratio as a function of the vertical pressure on bentonite immersed in distilled water and NaCl solution
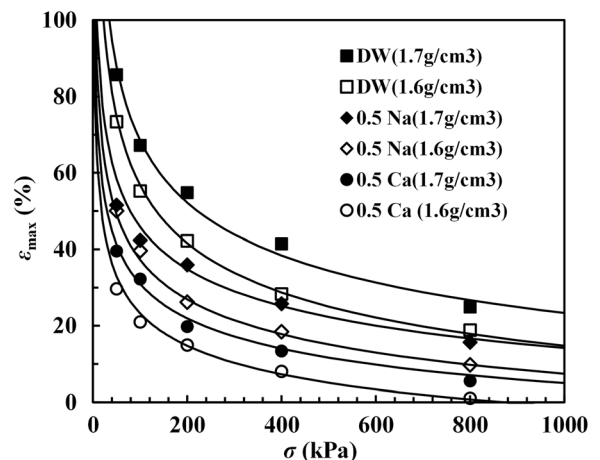

Fig. 6 Comparison between estimation of the maximum swelling strain and experimental data from specimens in various solutions

Predicted values indicated that under the same vertical pressure, montmorillonite void ratio was independent of the initial dry density of compacted bentonite. The initial dry density had a significant effect on maximum swelling strain.

CONCLUSION

The salt solution had significant effects on the swelling characteristics of bentonite. On the one hand, increasing osmotic suction of pore water acted as an extra effective stress component leading to a depression in swelling potential, which may explain the fact that the swelling strain decreased with increasing concentration of salt solution. On the other hand, the cation exchange reactions between the solution and bentonite also had a significant influence on swelling characteristics, as the swelling strains of GMZ bentonite in 1.0 M NaCl solution were larger than those in 0.5 M CaCl$_2$ solution, even the osmotic suction of the former solution was greater than that of the latter solution.

A modified swelling fractal model was developed to predict the swelling strains of compacted bentonite affected by salt solution. The effective stress incorporating osmotic suction was applied to describe the effect of salinity on swelling properties. And the swelling coefficient, K, was employed to take the effect of exchangeable cations into consideration, which can be calculated using the DDL model under osmotic swelling in distilled water. The modified fractal model offers an effective method to describe swelling characteristics of compacted bentonite in salt solution incorporating ion-exchange reactions.

ACKNOWLEDGEMENTS

REFERENCES

Åkesson, M., Jacinto, A. C., Gatabin, C., Sanchez, M., & Ledesma, A. (2009). Bentonite THM behaviour at high temperatures: Experimental and numerical analysis. *Geotechnique, 59*, 307–318.

ASTM. (2010). Standard test method for measuring the exchange complex and cation exchange capacity of inorganic fine-grained soils. *ASTM* D7503–D7510.

Avnir, D., & Jaroniec, M. (1989). An isotherm equation for adsorption on fractal surfaces of heterogeneous porous materials. *Langmuir, 5*, 1431–1433.

Birgersson, M. (2017). A general framework for ion equilibrium calculations in compacted bentonite. *Geochimica et Cosmochimica Acta, 200*, 186–200.

Bolt, G. H. (1956). Physico-chemical analysis of the compressibility of pure clays. *Géotechnique, 6*, 86–93.

Cadene, A., Durand-Vidal, S., Turq, P., & Brendle, J. (2005). Study of individual Na-montmorillonite particles size, morphology, and apparent charge. *Journal of Colloid and Interface Science, 285*, 719–730.

Casimir, H. B. C., & Polder, D. (1948). The influence of retardation of the London–van der Waals forces. *Physical Review, 73*, 360–372.

Celis, R., Cornejo, J., & Hermosin, M. C. (1998). Textural properties of synthetic clay-ferrihydrite associations. *Clay Minerals, 33*, 395–407.

Chen, Y. G., Cui, Y. J., Tang, A. M., Wang, Q., & Ye, W. M. (2014). A preliminary study on hydraulic resistance of bentonite/host-rock seal interface. *Géotechnique, 64*, 997–1002.

Chen, Y. G., Zhu, C. M., Ye, W. M., Cui, Y. J., & Chen, B. (2016). Effects of solution concentration and vertical stress on the swelling behavior of compacted GMZ01 bentonite. *Applied Clay Science, 124*, 11–20.

Dohrmann, R., Kaufhold, S., & Lundqvist, B. (2013). The role of clays for safe storage of nuclear waste. Pp. 677–710 in: *Handbook of Clay Science, Techniques and Applications* (F. Bergaya and G. Lagaly, editors). Developments in Clay Science, Vol. 5B, Elsevier, Amsterdam.

Ferrage, E. (2016). Investigation of the interlayer organization of water and ions in smectite from the combined use of diffraction experiments and molecular simulations. A review of methodology, applications, and perspectives. *Clays and Clay Minerals, 64*, 348–373.

Ferrage, E., Lanson, B., Sakharov, B. A., Geoffroy, N., Jacquot, E., & Drits, V. A. (2007). Investigation of dioctahedral smectite hydration properties by modeling of X-ray diffraction profiles: Influence of layer charge and charge location. *American Mineralogist, 92*, 1731–1743.

Holmboe, M., Wold, S., & Jonsson, M. (2010). Colloid diffusion in compacted bentonite: Microstructural constraints. *Clays and Clay Minerals, 58*, 532–541.

Iwata, S., Tabuchi, T., & Warkentin, B. P. (1988). *Soil–water interactions* (pp. 131–166). New York: Marcel Dekker, Inc..

Karnland, O., Olsson, S., Nilsson, U., & Sellin, P. (2007). Experimentally determined swelling pressures and geochemical interactions of compacted Wyoming bentonite with highly alkaline solutions. *Physics and Chemistry of the Earth Parts A/B/C, 32*, 275–286.

Kaufhold, S., & Dohrmann, R. (2016). Distinguishing between more and less suitable bentonites for high-level radioactive waste. *Clay Minerals, 51*, 289–302.

Liu, L. (2013). Prediction of swelling pressures of different types of bentonite in dilute solutions. *Colloids and Surfaces A Physicochemical and Engineering Aspects, 434*, 303–318.

Liu, L., & Neretnieks, I. (2008). Homo-interaction between parallel plates at constant charge. *Colloids and Surfaces A Physicochemical and Engineering Aspects, 317*, 636–642.

Rao, S. M., & Shivananda, P. (2005). Role of osmotic suction in swelling of salt-amended clays. *Canadian Geotechnical Journal, 42*, 307–315.

Rao, S. M., & Thyagaraj, T. (2007). Swell–compression behaviour of compacted clays under chemical gradient. *Canadian Geotechnical Journal, 44*, 520–532.

Saiyouri, N., Tessier, D., & Hicher, P. Y. (2004). Experimental study of swelling in unsaturated compacted clays. *Clay Minerals, 39*, 469–479.

Schramm, L. L., & Kwak, J. C. T. (1982a). Influence of exchangeable cation composition on the size and shape of montmorillonite particles in dilute suspension [J]. *American Journal of Hypertension, 12*(4), 41.

Schramm, L. L., & Kwak, J. C. T. (1982b). Influence of exchangeable cation composition on the size and shape of montmorillonite particles in dilute suspension. *Clays and Clay Minerals, 30*, 40–48.

Segad, M., Bo, J., & Cabane, B. (2012a). Tactoid formation in montmorillonite. *Journal of Physical Chemistry C, 116*, 25425–25433.

Segad, M., Hanski, S., Olsson, U., Ruokolainen, J., Åkesson, T., & Bo, J. (2012b). Microstructural and swelling properties of ca and na montmorillonite: (in situ) observations with Cryo-TEM and SAXS. *Journal of Physical Chemistry C, 116*, 7596–7601.

Sellin, P., & Leupin, O. (2013). The use of clay as an engineered barrier in radioactive waste management – A review. *Clays and Clay Minerals, 61*, 477–498.

Siddiqua, S. S., Blatz, J. B., & Siemens, G. S. (2011). Evaluation of the impact of pore fluid chemistry on the hydro-mechanical behavior of clay based sealing materials. *Canadian Geotechnical Journal, 48*, 199–213.

Sun, D. A., Zhang, J. Y., Zhang, J. R., & Zhang, L. (2013). Swelling characteristics of GMZ bentonite and its mixtures with sand. *Applied Clay Science, 83*, 224–230.

Sun, D. A., Zhang, L., Li, J., & Zhang, B. C. (2015). Evaluation and prediction of the swelling pressures of GMZ bentonites saturated with saline solution. *Applied Clay Science, 105*, 207–216.

Tripathy, S., Sridharan, A., & Schanz, T. (2004). Swelling pressures of compacted bentonites from diffuse double layer t. *Canadian Geotechnical Journal, 41*, 437–450.

Villar, M. V. (2006). Infiltration tests on a granite/bentonite mixture: Influence of water salinity. *Applied Clay Science, 31*, 96–109.

Villar, M. V., Martín, P. L., Romero, F. J., Iglesias, R. J., & Gutiérrez-Rodrigo, V. (2016). Saturation of barrier materials under thermal gradient. *Geomechanics for Energy and the Environment, 8*, 38–51.

Xiang, G. S., Xu, Y. F., & Jiang, H. (2014). Surface fractal dimension of bentonite and its application in calculation of swelling deformation. *Surface Review and Letters, 21*, 1450074.

Xiang, G. S., Xu, Y. F., Xie, S. H., & Fang, Y. (2016). A simple method for testing the fractal dimension of compacted bentonite immersed in salt solution. *Surface Review and Letters, 24*, 1750040.

Xu, Y. (2018). Fractal model for the correlation relating total suction to water content of bentonites. *Fractals, 26*, 1850028.

Xu, Y. F., Matsuoka, H., & Sun, D. A. (2003) Swelling characteristics of fractal-textured bentonite and its mixtures. *Applied Clay Science, 22*(4), 197–209.

Xu, Y., Xiang, G., Jiang, H., Chen, T., & Chu, F. (2014). Role of osmotic suction in volume change of clays in salt solution. *Applied Clay Science, 101*, 354–361.

Ye, W. M., Zhang, F., Chen, B., Chen, Y. G., Wang, Q., & Cui, Y. J. (2014). Effects of salt solutions on the hydro-mechanical behavior of compacted GMZ01 bentonite. *Environmental Earth Sciences, 72*, 2621–2630.

Ye, W. M., Zhu, C. M., Chen, Y. G., Chen, B., Cui, Y. J., & Wang, J. (2015). Influence of salt solutions on the swelling behavior of the compacted GMZ01 bentonite. *Environmental Earth Sciences, 74*, 793–802.

Yong, R. N. (1999). Soil suction and soil-water potentials in swelling clays in engineered clay barriers. *Engineering Geology, 54*, 3–13.

Zheng, L., Rutqvist, J., Birkholzer, J. T., & Liu, H. H. (2015). On the impact of temperatures up to, 200°C in clay repositories with bentonite engineer barrier systems: A study with coupled thermal, hydrological, chemical, and mechanical modeling. *Engineering Geology, 197*, 278–295.